β-Cell Mitochondria Exhibit Membrane Potential Heterogeneity That Can Be Altered by Stimulatory or Toxic Fuel Levels

Jakob D. Wikstrom,[1] Shana M. Katzman,[1] Hibo Mohamed,[1] Gilad Twig,[1] Solomon A. Graf,[1] Emma Heart,[2] Anthony J.A. Molina,[1] Barbara E. Corkey,[2] Lina Moitoso de Vargas,[2] Nika N. Danial,[3] Sheila Collins,[4] and Orian S. Shirihai[1]

OBJECTIVE—β-Cell response to glucose is characterized by mitochondrial membrane potential (ΔΨ) hyperpolarization and the production of metabolites that serve as insulin secretory signals. We have previously shown that glucose-induced mitochondrial hyperpolarization accompanies the concentration-dependent increase in insulin secretion within a wide range of glucose concentrations. This observation represents the integrated response of a large number of mitochondria within each individual cell. However, it is currently unclear whether all mitochondria within a single β-cell represent a metabolically homogenous population and whether fuel or other stimuli can recruit or silence sizable subpopulations of mitochondria. This study offers insight into the different metabolic states of β-cell mitochondria.

RESULTS—We show that mitochondria display a wide heterogeneity in ΔΨ and a millivolt range that is considerably larger than the change in millivolts induced by fuel challenge. Increasing glucose concentration recruits mitochondria into higher levels of homogeneity, while an in vitro diabetes model results in increased ΔΨ heterogeneity. Exploration of the mechanism behind heterogeneity revealed that temporary changes in ΔΨ of individual mitochondria, ATP-hydrolyzing mitochondria, and uncoupling protein 2 are not significant contributors to ΔΨ heterogeneity. We identified BAD, a proapoptotic BCL-2 family member previously implicated in mitochondrial recruitment of glucokinase, as a significant factor influencing the level of heterogeneity.

CONCLUSIONS—We suggest that mitochondrial ΔΨ heterogeneity in β-cells reflects a metabolic reservoir recruited by an increased level of fuels and therefore may serve as a therapeutic target. ***Diabetes*** **56:2569–2578, 2007**

From the [1]Department of Pharmacology and Experimental Therapeutics, Tufts University School of Medicine, Boston, Massachusetts; the [2]Obesity Research Center, Boston University School of Medicine, Boston, Massachusetts; the [3]Dana-Farber Cancer Institute, Harvard Medical School, Boston, Massachusetts; and the [4]Division of Translational Biology, Endocrine Biology Program, The Hamner Institutes for Health Sciences, Research Triangle Park, North Carolina.

Address correspondence and reprint requests to Orian S. Shirihai, Tufts University, Department of Pharmacology and Experimental Therapeutics, 136 Harrison Ave., Boston, MA 02111. E-mail: orian.shirihai@tufts.edu.

Received for publication 3 June 2006 and accepted in revised form 3 July 2007.

Published ahead of print at http://diabetes.diabetesjournals.org on 8 August 2007. DOI: 10.2337/db06-0757.

Additional information for this article can be found in an online appendix at http://dx.doi.org/10.2337/db06-0757.

S.M.K., H.M., and G.T. contributed equally to this study.

ΔΨ, mitochondrial membrane potential; FFA, free fatty acid; FI, fluorescence intensity; GLT, glucolipotoxicity; JC-1, tetrachloro-1,1′,3,3′-tetraethylbenzimidazol-carbocyanine-iodide; MeS; mono-methyl-succinate; MTG, MitoTracker Green; OM, oligomycin; PA-GFP$_{mt}$, matrix-targeted photo-activatable green fluorescent protein; ROS, reactive oxygen species; TMRE, tetramethylrhodamine-ethyl-ester-perchlorate; UCP2, uncoupling protein 2.

Mitochondria play essential roles in pancreatic β-cell function and dysfunction (1,2). They generate secretagogues for insulin secretion and produce factors that function to induce and propagate apoptosis. Essential to these processes is mitochondrial energy state, in the form of an electrochemical gradient, commonly termed the mitochondrial membrane potential (ΔΨ). This gradient influences ATP-to-ADP ratio, redox state (3–6), and reactive oxygen species (ROS), as well as calcium sequestration (2).

A growing body of evidence suggests that mitochondrial dysfunction plays a role in the pathophysiology of type 2 diabetes, both in the insulin secretion failure of β-cells and insulin resistance in peripheral tissues such as fat and skeletal muscle. Mitochondrial ATP production is cardinal in the pathway leading to insulin secretion, which is demonstrated in the diabetic phenotype of patients with mitochondrial DNA mutations (1,2). It is not known whether mitochondria in healthy or dysfunctional β-cells are metabolically homogeneous, thus having uniform ΔΨ, or whether they exist as subpopulations with different levels of ΔΨ, therefore contributing unevenly to ATP synthesis and insulin secretion. In theory, a heterogeneous population may represent the existence of subpopulations of mitochondria that have relatively reduced capacity to generate secretagogues and thus constitute a therapeutic target for increased insulin secretion. To date, the phenomenon of mitochondrial heterogeneity has been studied in several cell types (7–12) but not in β-cells.

ΔΨ reflects mitochondrial fuel availability, Kreb's cycle and respiratory chain activity, and processes that consume the proton gradient, including uncoupling and ATP synthesis. Glycolytic pathways supply the mitochondria with anapleurotic intermediates that participate in fuel-stimulated insulin secretion (1). BAD, a proapoptotic BCL-2 family member, has recently been implicated in cellular respiration (13). BAD is thought to interact with the mitochondrial glucokinase (hexokinase IV) complex, and BAD knock-out rodents exhibit reduced mitochondrial glucokinase activity (13). The uncoupling protein 2 (UCP2) has been shown to be a regulator of ΔΨ in β-cells (14). Alterations in UCP2 expression levels have been shown to modify β-cell ΔΨ (15,16), ATP levels, and the secretory response to glucose (17,18,19).

To test whether β-cell mitochondria constitute a metabolically diverse population, we developed a methodology that enabled the quantification of ΔΨ heterogeneity. By using this approach, we also determined its physiological relevance and systematically examined possible sources

of heterogeneity. We show that β-cell mitochondria are metabolically diverse and that the span of heterogeneity is considerably larger than fuel-induced changes in ΔΨ. Furthermore, we demonstrate that mitochondria become more heterogeneous in an in vitro diabetes model and more homogenous under acute fuel challenge. Finally, we found that cells from animals lacking BAD, but not UCP2, have an altered status of ΔΨ heterogeneity.

RESEARCH DESIGN AND METHODS

Twelve-week-old male C57BL6 mice, including wild-type (WT), BAD$^{-/-}$, and UCP2$^{-/-}$, were used. BAD and UCP2 deficiency has been previously described (20,21). Animals were fed a normal diet and were maintained under controlled conditions (a constant temperature [19–22°C] and a 14:10-h light-dark cycle) until death by CO_2 asphyxiation. All procedures were performed in accordance with the Tufts University Institutional Guidelines for Animal Care (IACUC no. 1104) in compliance with U.S. Public Health Service Regulation.

Islet isolation and primary cell culture. Islets of Langerhans were isolated as previously described (5) and the islet cells dispersed by treatment with Ca^{2+}/Mg^{2+}-free PBS supplemented with 0.05 mg/ml trypsin (Gibco, Grand Island, NY) with occasional agitation. Dispersed cells were plated on poly-D-lysine–coated glass slide–bottom dishes (MatTek, Ashland, MA) in RPMI-1640 culture media (Gibco) supplemented with 10 mmol/l glucose, 10% FCS (HyClone, South Logan, UT), 100 IU/ml penicillin (Gibco), and 100 μg/ml streptomycin (Gibco). Experiments were performed on individual cells not in contact with other cells after culture for 2–3 days at 37°C in a humidified atmosphere containing 5% CO_2. Before experiments, cells were kept in 3 mmol/l glucose for 4 h. In glucolipotoxicity (GLT) experiments, normal cells were kept in medium containing 20 mmol/l glucose, 0.4 mmol/l palmitate, and 0.5% BSA for 24 h before imaging (22). Analysis of 534 dispersed islet cells from two preparations revealed that 93% of cells that respond to increase in glucose from 3 to 8 mmol/l by mitochondrial hyperpolarization also stain positive for insulin by immunofluorescence (supplemental Fig. S1 [available in the online appendix at http://dx.doi.org/10.2337/db06-0757]). This is supported by a previous study examining the autofluorescence of flavins that confirmed that β-cells but not α-cells show a mitochondrial metabolic response to glucose (23). We therefore used the criterion of mitochondrial hyperpolarization to determine the identity of β-cells at the end of each analysis. In the heterogeneity experiments, 23% of the cells did not show mitochondrial hyperpolarization in response to glucose. The cause for this in our experiments is not clear, although glucose unresponsiveness has been reported previously (24), and our control experiments indicate a higher fraction of non–β-cells within this fraction.

Fluorescent probes. While measuring ΔΨ with the potentiometric dye tetrachloro-1,1′,3,3′-tetraethylbenzimidazol-carbocyanine-iodide (JC-1), cells were incubated for 5 min at a concentration of 1 μmol/l. Tetramethylrhodamine-ethyl-ester-perchlorate (TMRE) and MitoTracker Green FM (MTG) were used at concentrations of 7 and 100 nmol/l, respectively, and cells were incubated for 1.5 h before imaging. TMRE was kept in the medium throughout the experiments, while MTG was removed before imaging. All dyes were obtained from Molecular Probes (Eugene, OR).

Confocal microscopy. Experiments were performed on live cells using a Zeiss LSM 510 Meta microscope (Carl Zeiss, Oberkochen, Germany) with a 100× oil immersion objective. TMRE was excited with a 543-nm helium/neon laser and emission recorded through a band-pass 650- to 710-nm filter. MTG was excited using a 488-nm argon laser, and emission was recorded through a band pass 500- to 550-nm filter. During the experiments, cells were kept at 37°C in a humidified atmosphere containing 5% CO_2. To allow for cellular response and dye equilibration, imaging was paused for 10 min after change in fuel concentration. Scanning cells continuously for 45 min did not induce any change in TMRE fluorescence intensity (FI), thus indicating minimal levels of phototoxicity.

Tracking single mitochondria. A matrix-targeted photo-activatable green fluorescent protein (PA-GFP$_{mt}$) was expressed in β-cells using adenoviral transfection. Expression was derived by rat insulin promoter. Cloning and production of the virus was accomplished using the two-cosmid system (25). Briefly, the DNA coding for photo-activatable green fluorescent protein was fused to a mitochondrial targeting sequence. Subsequently, it was subcloned into an adenovirus shuttle vector (pLEPMV10) used for the generation of DNA cosmid through recombination in DH5α bacteria. Replication deficient viral particles were packaged in HEK293 cells and CsCl purified (26). Tracking of ΔΨ in individual mitochondria was performed in dispersed β-cells stained with TMRE 72 h after transfection with PA-GFP$_{mt}$ (Fig. 3*A*), described in detail previously (27). A transition to its active (fluorescent) form was achieved by photo-isomerization using a 2-photon laser (750 nm) to give a 375-nm photon equivalence at the focal plane. This allowed for selective activation of regions <0.5 μm^2. Z-stack time-lapse imaging was performed to follow individual mitochondria and correct for their movements.

ΔΨ analysis. Different mitochondria appear in different focal planes and therefore exhibit a false variability in dye FI in confocal microscopy images. To correct for this we used the ratio of red to green, where the green signal (MTG) was a membrane potential–independent signal and the red signal (TMRE) was membrane potential sensitive. The Nernst equation allows conversion of FI values, which reflect dye concentration distributions over the mitochondrial membranes, into absolute millivolt values. By applying modified versions of this equation, we were able to calculate a cell's relative change in ΔΨ and the relative ΔΨ of a single mitochondrion. Further, an adapted Nernst equation was used to determine the SD of potentials derived at each and every pixel in an image, thereby giving a value of ΔΨ heterogeneity. For a detailed description of the ΔΨ calculation theory and application, see the supplements available in the online appendix.

Statistical analysis. Data are given as means ± SEM. Two-tailed, unpaired, or paired Student's *t* tests were used to compare cells of different types or under different fuel concentrations.

RESULTS

Mitochondria in pancreatic islets are metabolically heterogeneous. To test for metabolic heterogeneity in the mitochondria of pancreatic islets, we used the fluorescent probe JC-1. Increasing ΔΨ negativity (hyperpolarization) shifts the JC-1 signal from green to red (9). JC-1 revealed a distinct heterogeneity in ΔΨ, as shown in Fig. 1*A*. A subpopulation of mitochondria stained red and thus have a higher ΔΨ than their green counterparts. Similar diversity was observed in both dispersed islet cells and cells that were part of intact islets ($n = 9$ experiments).

A quantification approach to single-cell mitochondrial metabolic heterogeneity. To further characterize heterogeneity in ΔΨ, we set out to quantify it in millivolts. Quantification of ΔΨ heterogeneity in millivolts enables comparison of mitochondria's metabolic status within and between cells and monitoring of how it changes with the type of extra cellular environment. To get a functional perspective, we also sought to determine the single β-cell response to fuel challenge in millivolts. JC-1 proved inadequate for these experiments due to its relatively slow response time to changes in ΔΨ (28). Additionally, JC-1 does not allow quantitative analysis of ΔΨ in millivolts due to its bimodal fluorescence and is prone to bleaching after only moderate laser exposure.

We developed a ratiometric imaging approach using dual staining with the ΔΨ-dependent probe TMRE and the ΔΨ-independent dye MTG (7). Importantly, TMRE equilibration is rapid due to high permeability across membranes and it does not inhibit mitochondrial respiration in low concentrations (29). The dye concentrations used are lower than those previously reported in intact cell studies (7,8,29,30,31). This enabled minimal levels of cytotoxicity and self-quenching of the dyes. To establish ΔΨ dependency of TMRE and rule out ΔΨ sensitivity of MTG, we performed two types of experiments. The effect of the proton ionophore FCCP [carbonyl cyanide 4-(trifluoromethoxy)phenylhydrazone] on MTG and TMRE was tested in dispersed β-cells. FCCP strongly reduced TMRE fluorescence but left MTG fluorescence virtually unchanged (Fig. 1*B*). Glucose exposure greatly enhanced TMRE FI but elicited a relatively small change in MTG fluorescence (Fig. 1*C*).

Since TMRE and MTG signals are similarly influenced by changes in focal plane, the ratio product, TMRE/MTG, retains the voltage dependency of TMRE and is independent of the exact focal plane. Figure 1*D* demonstrates this

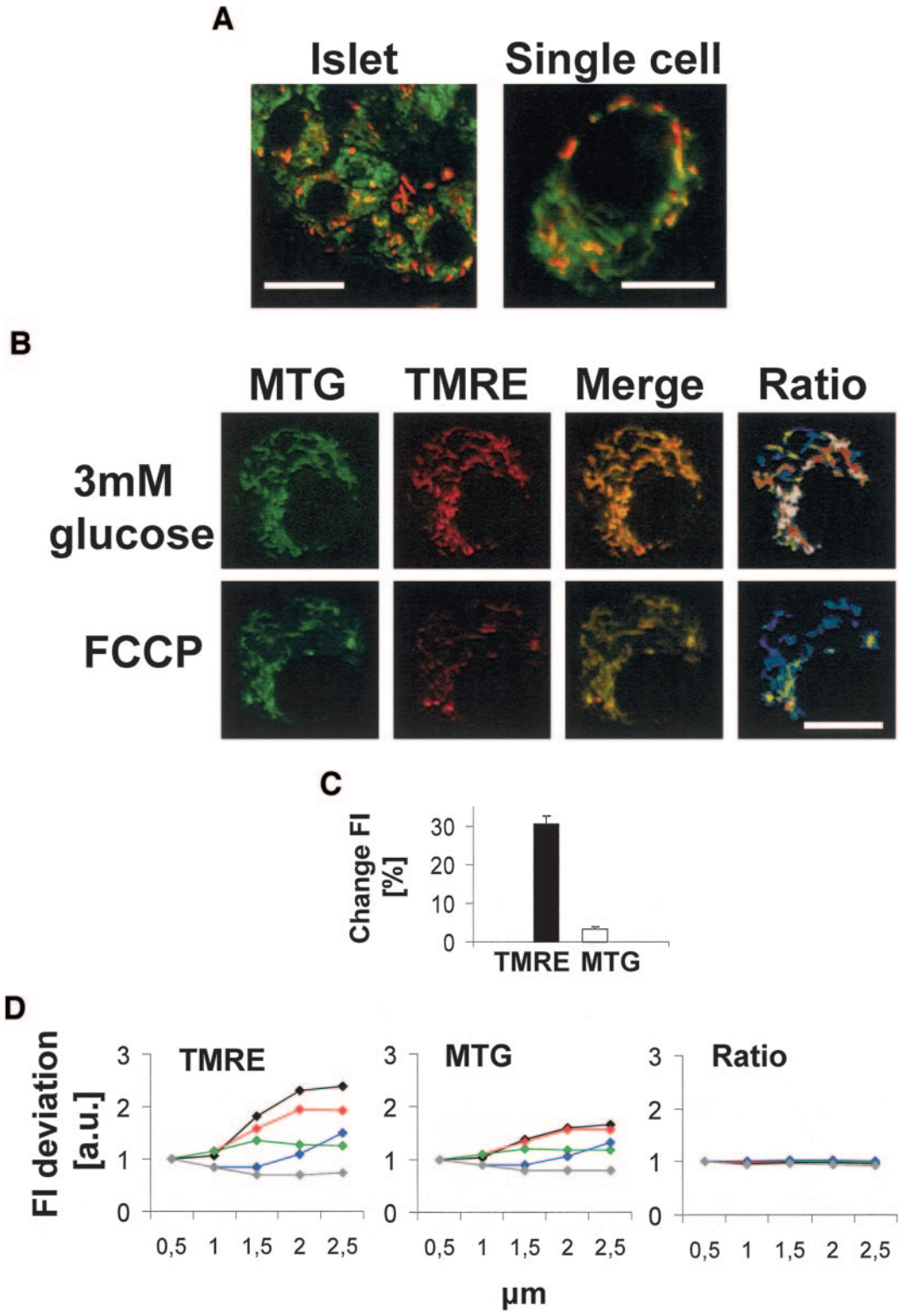

FIG. 1. ***A*****: Metabolic heterogeneity of mitochondria. Confocal microscopy images of cells in an intact pancreatic islet (*left*) and a dispersed cell (*right*) stained with the potentiometric mitochondrial dye JC-1. Hyperpolarized mitochondria appear as red and depolarized as green. Note the existence of a hyperpolarized subpopulation of mitochondria. Scale bars = 10 (*left*) and 5 (*right*) µm. *B*: FCCP virtually abolishes TMRE fluorescence but leaves MTG virtually intact. Dispersed β-cells were simultaneously stained with TMRE (red) and MTG (green). After imaging at basal glucose (3 mmol/l) (*top row*), 1 µmol/l of the uncoupling agent FCCP was added and cells were imaged after 10 min (*bottom row*). Merged images were generated by superimposing the red and green images. Ratio images were produced by calculating the ratio of FI (TMRE-to-MTG) of each individual pixel and colour labelling accordingly using the image analysis software. Scale bar = 5 µm. *C*: Glucose-induced change in FI of TMRE and MTG. Dispersed β-cells were double stained with TMRE and MTG and imaged at low (3 mmol/l) and high (8 mmol/l) glucose concentrations. The bars denote the relative change in FI under 8 compared with 3mmol/l glucose (n = 45 cells). *D*: The use of the TMRE-to-MTG ratio reduces the variability in FI with focal plane. Dispersed β-cells were imaged at 3 mmol/l glucose by using the Z-stack function of the confocal microscope, with a distance of 0.5 µm between the 5 sections, thus creating 5 series of 5 data points (n = 5 cells). The relative FI of TMRE, MTG, and the TMRE-to-MTG ratio were plotted against the Z-plane. Each colored line represents one cell.**

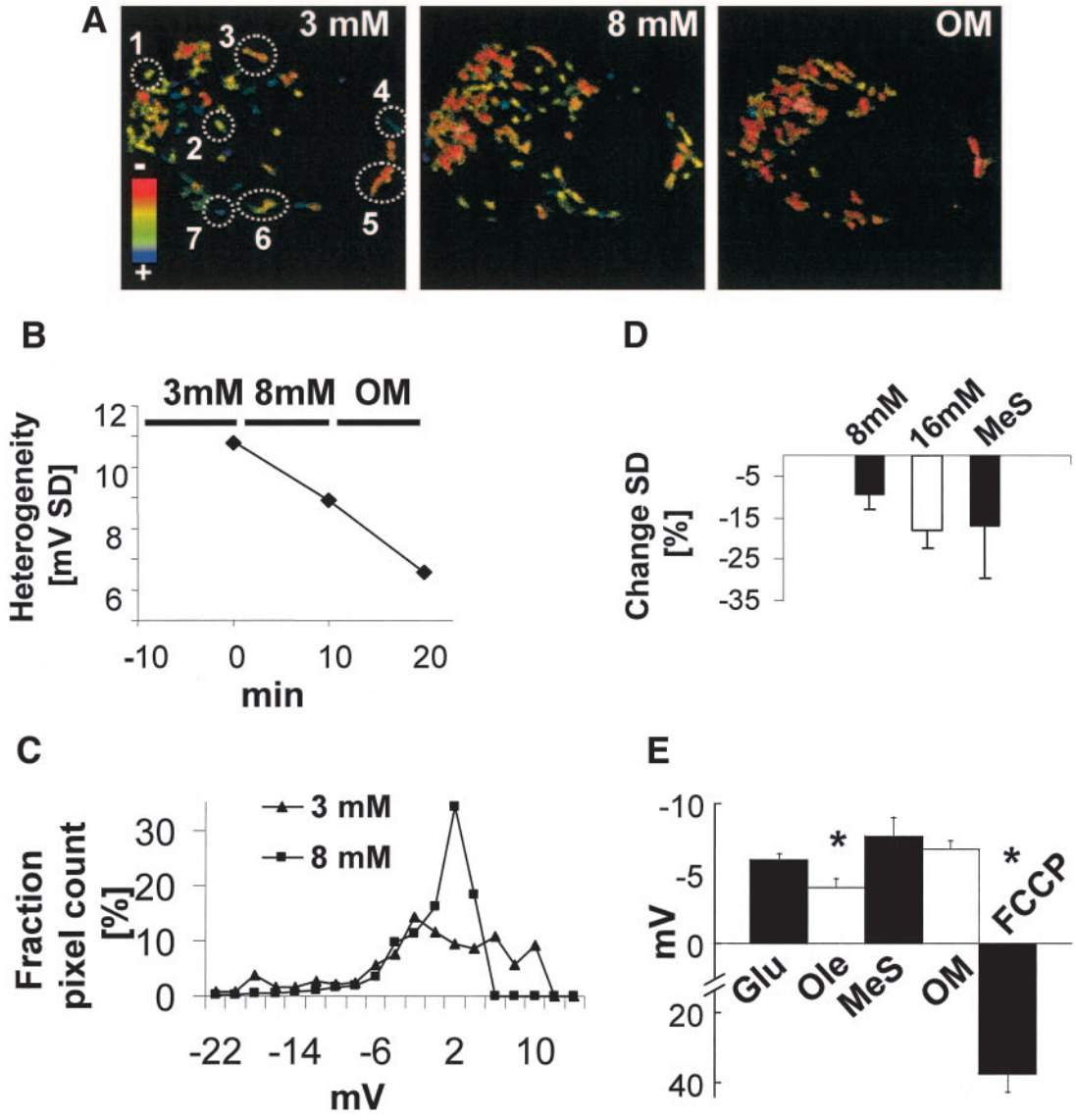

FIG. 2. *A*: Mitochondria in dispersed β-cells show heterogeneity in Δψ. Representive pseudo-color images of TMRE-to-MTG ratio of a cell imaged in glucose concentrations of 3, 8, and 8 mmol/l with 1 μmol/l OM. As indicated by the color bar, hyperpolarized mitochondria appear red, while depolarized appear blue. The ΔΨ of each mitochondria (encircled) was calculated in reference to the average ΔΨ of all mitochondria in the cell using a modified version of the Nernst equation (online supplement, Equation 2): 1, −1.5 mV; 2, 3.8 mV; 3, −6.4 mV; 4, −12.8 mV; 5, 5.8 mV; 6, −0.7 mV; and 7, −20.5 mV. Scale bar = 5 μm. *B*: The distribution of Δψ narrows with glucose and OM. Heterogeneity was measured before and after glucose and OM challenge (same cell as in Fig. 3*A*). The ratio (MTG-to-TMRE) FI of each individual pixel was determined and the SD of the Δψ calculated (online supplement, Equation 3). *C*: Effect of fuel challenge on the distribution range of heterogeneity in Δψ of a dispersed β-cell (online supplements, Equation 3). Triangles and squares indicate distribution at 3 (SD 8.2) and 8 mmol/l (SD 4.6) glucose, respectively. The millivolt values were binned at a 2-mV interval. Relative pixel frequency of each millivolt interval is indicated on the *y*-axis. *D*: Mean decrease in heterogeneity (lower SD) in ΔΨ with fuel challenge. WT dispersed β-cells were kept at 3 mmol/l glucose, and fuel challenge was set as elevation of glucose concentration to 8 mmol/l (n = 11 cells) or 16 mmol/l (n = 7 cells) or addition of 15 mmol/l MeS (n = 9 cells). All data points were statistically significant compared with 3 mmol/l. *E*: Fuel-induced change in Δψ of dispersed β-cells. Change in Δψ was measured for 5 different stimuli (online supplement, Equation 1), as follows: *1*) elevation in glucose concentration from 3 to 8 mmol/l (Glu) (n = 49 cells), *2*) 0.3 μmol/l oleate added on top of glucose that had previously been increased from 3 to 8 mmol/l (Ole) (n = 14 cells, P <0.05), *3*) 15 mmol/l MeS added to normal cells in 3 mmol/l glucose (MeS) (n = 13 cells, P < 0.05), *4*) 1 mmol/l OM added to normal cells in 8 mmol/l glucose (OM) (n = 39 cells, P <0.05), and *5*) 1 μmol/l FCCP added to normal cells in 8 mmol/l glucose and 1 μmol/l OM (FCCP) (n = 13 cells, P < 0.0001). P values were calculated by comparing with the baseline values of the cell and by comparing between the different agents. The significant P values of the latter are indicated by *.

effect in 5 cells of 31 that were studied in five sections along their *Z*-axes. While the FI of TMRE and MTG is highly variable, the TMRE-to-MTG ratio is essentially independent of focal plane. For details of the image analysis and algorithms used to calculate ΔΨ, see the online appendix supplement.

Mitochondrial metabolic heterogeneity in β-cells. Staining dispersed β-cells with TMRE and MTG revealed a cellular heterogeneity in ΔΨ similar to that observed with JC-1 (Fig. 2*A*). To illustrate the heterogeneity in a specific cell, we extracted the FI value of randomly chosen mitochondria and compared them to the mean FI of all the mitochondria within the cell by applying a modified version of the Nernst equation (online appendix supplement, Equation 2). The range of ΔΨ among the mitochondria in Fig. 2*A* was 26.3 mV, indicative of major differences in ATP production capacity.

To enable statistical analysis of ΔΨ heterogeneity, we

compared the FI of each image pixel to the mean FI of the mitochondria of the entire cell and calculated the $\Delta\Psi$ in millivolts per pixel. In doing so, we were able to determine the SD of all the pixels' $\Delta\Psi$, thereby creating a value of heterogeneity for each cell (online appendix supplement, Equation 3). By using this image analysis algorithm, it was ascertained that the pixels analyzed were of mitochondrial origin and not background staining. The SD of the cell in Fig. 2*A* was calculated to be 10.8 mV at 3 mmol/l glucose, translating into 95% of the mitochondria possessing $\Delta\Psi$ within a span of 43.2 mV (4 SD). The mean SD for multiple cells at 3 mmol/l glucose was determined to be 8.7 mV ($n = 27$ cells); 95% of analyzed pixels represent a span of 34.8 mV (4 SD).

To derive an estimation of the impact of such heterogeneity on ATP production, mitochondria of dispersed β-cells in 3 mmol/l glucose were divided into two groups in such way that the mean FI of the hyperpolarized group ($n = 56$) was 7.1 mV higher than the mean of the depolarized group ($n = 32$). A difference of 7.1 mV translates to a fivefold difference in ATP synthesis capacity (6). Based on this analysis, it is estimated that the depolarized group comprises 36% of the mitochondria in the β-cell.

Fuels modulate the functional distribution of mitochondria. Higher fuel levels induce higher rates of oxidative phosphorylation in mitochondria. We recently showed that mean $\Delta\Psi$ in β-cells increases linearly with glucose concentration (5). In this study, we questioned whether the subpopulation of mitochondria with relatively low $\Delta\Psi$ can be recruited into a more active pool to handle fuel challenge. This would consequently decrease heterogeneity in $\Delta\Psi$ of the cell. Alternatively, if all mitochondria increase their $\Delta\Psi$ uniformly, the range of heterogeneity should remain constant. As a control to glucose, we used oligomycin (OM), known to hyperpolarize mitochondria.

Mitochondria in a normal dispersed β-cell responded to higher levels of glucose and to OM with hyperpolarization and increased $\Delta\Psi$ homogeneity (Fig. 2*B*). A typical β-cell (Fig. 2*C*) decreased its $\Delta\Psi$ SD span from 8.2 to 4.6 mV after glucose was elevated from 3 to 8 mmol/l. To test for a dose-response effect, we evaluated the effect of two stimulatory glucose concentrations. In normal dispersed β-cells, we found a significant mean decrease in heterogeneity value of 9.5 and 17.9% after elevation of glucose from 3 to 8 mmol/l and 3 to 16 mmol/l, respectively ($P < 0.05$; Fig. 2*D*). The magnitudes of SD change induced by the two different glucose concentrations were statistically indistinguishable ($P > 0.05$). $BAD^{-/-}$ cells exhibited a significant decrease in SD of 21.2% when exposed to 8 mmol/l glucose ($P < 0.05$), not significantly different from the WT (data not shown). $UCP2^{-/-}$ cells did not show any significant decrease in SD ($P > 0.05$; data not shown).

To investigate whether different mitochondrial populations have different capacities to import and metabolize various fuels, we tested the effect of mono-methyl-succinate (MeS), which bypasses glycolysis and feeds directly into the Kreb's cycle. We found a significant decrease in SD of 17.1% ($P < 0.05$) in cells after MeS challenge (data not shown). There was no significant difference when MeS challenge was compared with glucose challenge (Fig. 2*D*), indicating that premitochondrial glycolytic metabolism does not cause heterogeneity in $\Delta\Psi$.

Quantification of the global cellular fuel response in millivolts. Our results indicate that mitochondrial heterogeneity spans a range of ~35 mV (Fig. 4). However, the actual change in millivolts in response to different fuels is not known. To better understand the physiological significance of mitochondrial heterogeneity, it is necessary to measure the change in millivolts. To determine the fuel response in millivolts, we measured the increase in FI of β-cell mitochondria (Fig. 2*E*). Using a modified version of the Nernst equation, we translated the change in FI to a Δ millivolts value for every cell (online appendix supplement, Equation 1). Figure 2*E* shows a mean response of $\Delta\Psi$ after an increase in glucose concentration from 3 to 8 mmol/l of −6.0 mV. A total of 77% (49 of 64) of the dispersed β-cells responded to glucose by elevation of $\Delta\Psi$ (threshold −2.0 mV), and only those were used for the analysis, since glucose-induced hyperpolarization is a characteristic of β-cells (RESEARCH DESIGN AND METHODS and 23).

Addition of 0.3 mmol/l oleate to 8 mmol/l glucose resulted in further hyperpolarization of −4.0 mV in dispersed β-cells (Fig. 2*E*). This increase was significantly smaller than the glucose response of the same cells ($P < 0.05$). Only the cells responding to oleate (13 of 33) were included in the analysis.

To examine whether the magnitude of hyperpolarization would differ after bypassing glycolysis, we tested the effect of MeS on the dispersed β-cells. The average response to MeS (−7.7 mV) was not significantly different from the response to glucose (Fig. 2*E*).

Tracking subcellular $\Delta\Psi$ differences over time. Heterogeneity may represent a state in which each individual mitochondrion's $\Delta\Psi$ is unstable or, alternatively, a state in which the $\Delta\Psi$ of each mitochondrion is stable but the population is diverse. Therefore, to elucidate the mechanism behind $\Delta\Psi$ heterogeneity, there is a need to follow the $\Delta\Psi$ of individual mitochondria over time. We tagged individual mitochondria within the intact cell by photoconverting $PA\text{-}GFP_{mt}$ and monitored $\Delta\Psi$ by costaining with TMRE. $PA\text{-}GFP_{mt}$ is diffusible only within the mitochondrial matrix and therefore delineates the matrix boundary of each mitochondria in which it has been photo-converted (27). Like MTG, it can be used in conjunction with TMRE for ratiometric measurement of $\Delta\Psi$ (online supplement, Equation 4). Six experiments in which two or three mitochondria in a dispersed β-cell were photo-labeled and tracked for 20–30 min are shown in Fig. 3*A* and *B*. Comparable results were recorded from INS1 cells (rat insulinoma cell line; online supplement, Fig. S3*C*–*E*). Observation of single mitochondria for longer than 20–30 min is difficult to achieve due to the occurrence of fusion and fission events. Nevertheless, during a period of up to 30 min, the $\Delta\Psi$ held relatively stable (SD 1.6 mV; online supplement, Fig. S3*D*–*E*). This suggests that $\Delta\Psi$ heterogeneity in β-cells is not due to intrinsic temporal changes in $\Delta\Psi$ in each individual mitochondria but rather supports the existence of subpopulations of mitochondria possessing different $\Delta\Psi$.

Mechanism of $\Delta\Psi$ heterogeneity. The proton gradient across the inner mitochondrial membrane is built up by proton efflux from the matrix and is dissipated either through the F1FO-ATPsynthase or by alternative routes such as uncoupling proteins. To investigate the cause of heterogeneity, we undertook a systematic approach examining metabolic events both upstream and downstream of the gradient.

Role of UCP2. UCP2 has been shown to be both induced and activated by ROS and free fatty acids (FFAs) (14,32). We hypothesized that a heterogeneous allocation or activ-

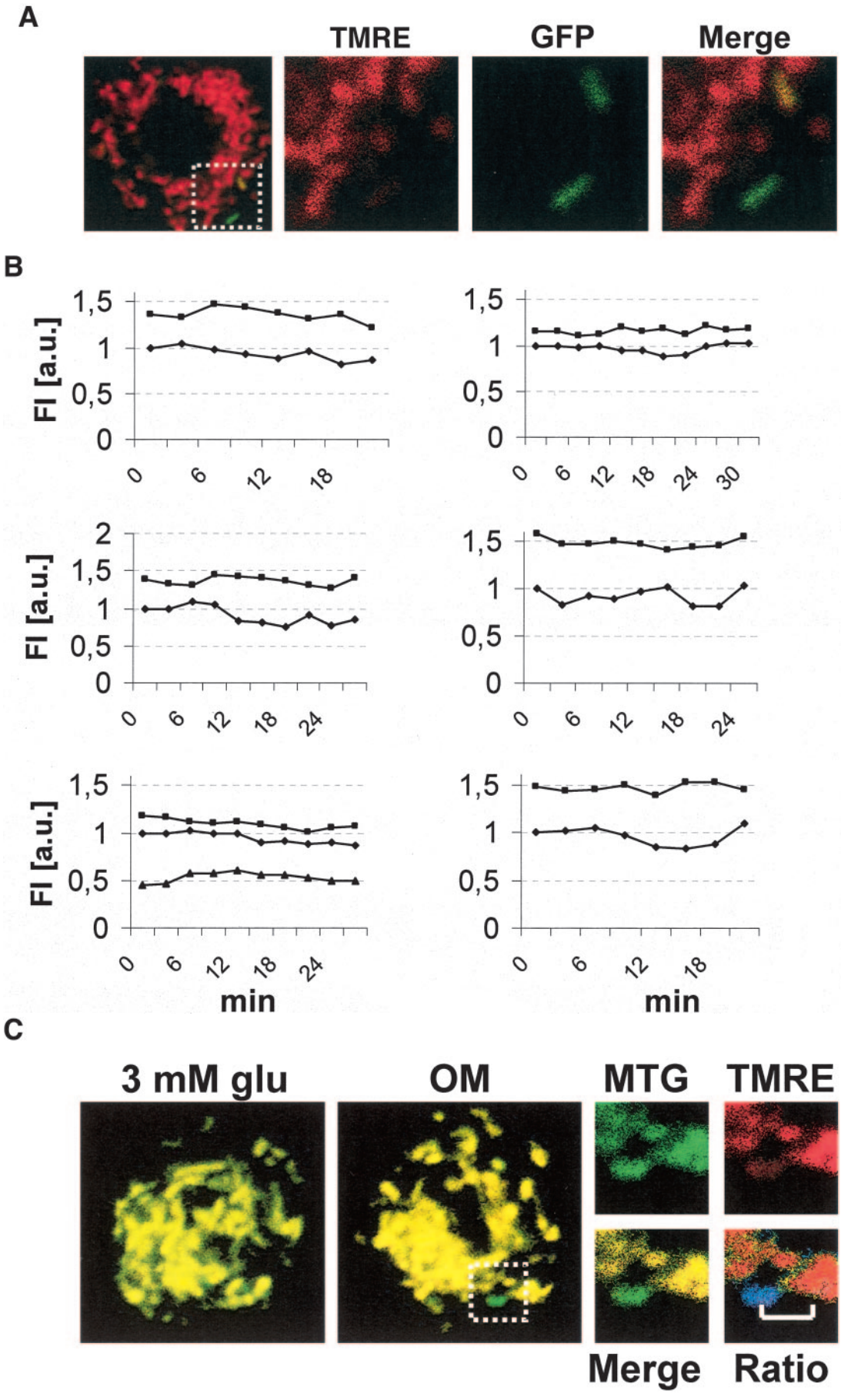

FIG. 3. Tracking Δψ in individual β-cell mitochondria using TMRE and PA-GFP$_{mt}$. *A*: Mitochondria with different TMRE staining were labelled by photo-activation. *B*: ΔΨ was monitored by time lapse imaging. *C*: ATP-hydrolyzing mitochondria are minor contributors to Δψ. A dispersed β-cell imaged at 3 mmol/l glucose, before and after addition of 1 μmol/l OM. Only one mitochondrion depolarized, equivalent to ~1% of the mitochondrial area in the confocal image section. Bar indicates a potential difference of 28 mV between the depolarized mitochondrion (blue) and its neighbour (online supplement, Equation 4).

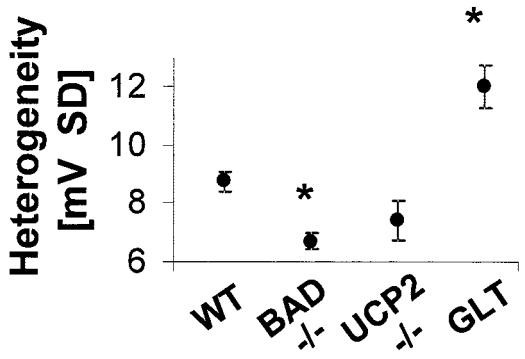

FIG. 4. Analysis of potential contributors to ΔΨ subcellular heterogeneity. Dispersed β-cells were imaged as in Fig. 3*A* and the mean SD of the pixel ΔΨ distribution calculated. WT, BAD$^{-/-}$, and UCP$^{-/-}$ cells were studied at 3 mmol/l glucose. GLT conditions (20 mmol/l glucose, 0.4 mmol/l palmitate) were kept for 24 h. *Statistically significant change from WT at 3 mmol/l glucose.

ity of UCP2 among mitochondria might affect the heterogeneity in ΔΨ. Dispersed β-cells from mice deficient in UCP2 were tested for heterogeneity. We found a slightly reduced ΔΨ heterogeneity level in UCP2$^{-/-}$, but this was not statistically significant compared with the WT ($P = 0.12$, $n = 9$ cells; Fig. 4).

Role of BAD. As BAD has been implicated in cellular respiration, a heterogeneous distribution or activity of mitochondrial BAD could result in heterogeneous fuel input to different mitochondria. We therefore examined dispersed BAD-deficient β-cells as described above for the WT cells. The mean ΔΨ SD in BAD$^{-/-}$ cells was determined to be 6.7 mV (Fig. 4), a decrease of 23% compared with WT cells ($P < 0.001$). Comparable differences were observed in two separate batches of BAD-deficient mice ($n = 6$ and 11 cells).

ATP-hydrolyzing mitochondria. ΔΨ may be maintained by either proton efflux from the matrix by the respiratory chain or by reversed F1FO-ATPsynthase activity resulting in ATP consumption instead of production (33). Such ATP-hydrolyzing mitochondria would be expected to have a different ΔΨ than their ATP-producing counterparts. To account for ATP-hydrolyzing mitochondria as a possible cause of heterogeneity in ΔΨ, we inhibited the F1FO-ATPsynthase with OM. In theory, OM would cause ATP-producing mitochondria to hyperpolarize and ATP-consuming mitochondria to depolarize. In Fig. 3*C*, we show that the majority of the mitochondria in a dispersed β-cell hyperpolarize in response to OM, while one mitochondrion depolarizes. A minority of the cells treated with OM exhibited ATP-consuming mitochondria (36%), with an average of 2.6 mitochondria (SE 0.6) covering a mean mitochondrial area of 4.0% (SE 1.3) per confocal image section ($n = 44$ cells). The infrequency of ATP-consuming mitochondria does not support a major contribution to ΔΨ heterogeneity.

Subcellular localization. In HeLa cells, it has been reported that peripheral mitochondria have a higher ΔΨ than perinuclear mitochondria, suggesting the possibility that heterogeneity may represent differences in ΔΨ that originate from localization (7). To test for this relationship in dispersed β-cells, we measured the FI in perinuclear (defined as juxtaposed to the nucleus) and peripheral (defined as juxtaposed to the plasma membrane) mitochondria. We found no significant disparity in ΔΨ (average FI [arbitrary units] 570 ± 21 and 561 ± 35, respectively).

Contribution of imaging technique and sample preparation to heterogeneity. To exclude artifact influence on the measurements of heterogeneity, a series of control experiments were performed. Accounting for variability due to imaging, time laps measurements of mitochondrial heterogeneity showed minimal variation (online supplement, Fig. S3*A*). Comparison of perinuclear and peripheral mitochondria, as well as fluorescent beads (online supplement, Fig. S3*B*), showed little variation, thus indicating low spatial variability in measurements due to light scattering or uneven excitation/detection within the imaging field. To account for the contribution of damage during islet and cell isolation, parameters of mitochondrial damage and heterogeneity were compared between cells within the islets and in dispersed cells. No mitochondrial swelling was observed due to dispersion or GLT (online supplement, Fig. S2*A* and *B*). Heterogeneity was found in both whole islets and dispersed cells (Fig. 1*A*). Additionally, the INS1 cell line cells showed similar patterns of heterogeneity (online supplement, Fig. S2*C*).

TMRE may become diluted in damaged mitochondria that go through swelling even if actual membrane potential does not drop. To rule out such false-positive interpretations of ΔΨ depolarization in large mitochondria, the correlation between mitochondrial size and ΔΨ was studied. Depolarized mitochondria were found to be smaller than the average, which is expected since fragmentation is triggered by depolarization (34). Additionally, conditions with high levels of heterogeneity did not have increased mitochondrial diameter (Fig. 4).

Concerning overall noise estimation, changes of ΔΨ of the individual mitochondrion over time generate an SD of 1.6 mV ($n = 11$ individual mitochondria in 11 different cells and 60–160 data points per mitochondrion). If all mitochondria had similar baseline ΔΨ, it is expected that a population of ~100 mitochondria sampled at a single snapshot would create an SD of 1.97 mV. (SD is higher due to smaller sample size when a snapshot rather than a time-lapse is analyzed.) This value should be considered as the noise of the methodology (Fig. 3*A* and online supplement S3*E*).

Mitochondrial heterogeneity in β-cell dysfunction. We hypothesized that increased mitochondrial heterogeneity could be a characteristic of mitochondrial dysfunction in diabetic β-cells. To mimic diabetic conditions, we used a rich nutrient environment model (GLT), a previously described in vitro model of type 2 diabetes (22). WT dispersed β-cells were incubated in the presence of high glucose and high FFAs (RESEARCH DESIGN AND METHODS) and the effect on ΔΨ heterogeneity assessed. The mean ΔΨ SD was determined to be 11.9 mV, a significant increase of 37% compared with normal cells ($P < 0.001$; Fig. 4). The cell's morphology was maintained, and the mitochondria appeared hyperpolarized and of normal size (online supplement, Fig. S2*B*).

To explore whether ATP-consuming mitochondria become more abundant in cells under GLT conditions and thus affect the level of heterogeneity, we inhibited the F1FO-ATPsynthase with OM to reveal any such mitochondria. No difference in ΔΨ heterogeneity was observed in cells under OM, indicating that ATP-consuming mitochondria are not a significant contributor to the level of heterogeneity observed under GLT (data not shown).

DISCUSSION

This study examines the diverse metabolic state of β-cell mitochondria. We show that mitochondria within the β-cell are metabolically heterogeneous and that their ΔΨ spans a range larger than the change of ΔΨ in millivolts induced by fuel challenge. Increasing glucose concentration recruits mitochondria into a higher level of homogeneity, while chronic exposure to GLT results in increased heterogeneity. Exploration of the mechanism behind heterogeneity revealed that transient changes in ΔΨ of individual mitochondria, ATP-hydrolyzing mitochondria, and UCP2 are not significant contributors to ΔΨ heterogeneity. We identified BAD, previously implicated in mitochondrial recruitment of glucokinase, as a significant factor that influences the level of heterogeneity.

Implications of ΔΨ heterogeneity. We found that mitochondria in dispersed β-cells exhibit a considerable heterogeneity in ΔΨ, spanning >15 mV at normal glucose concentrations (Figs. 1*A*, 2*A–C*, and 4). This phenomenon may be of particular importance in β-cells, as ΔΨ drives ATP synthesis and hence influences ATP-sensitive K^+ channel activity and insulin secretion (2). Nicholls (6) reported that for every 14-mV decrease in ΔΨ, mitochondrial ATP production decreases 10-fold; the disparity in ATP production between hyper- and depolarized β-cell mitochondria consequently may exceed 10-fold.

Three fuels, glucose, MeS, and oleate, resulted in mitochondrial hyperpolarization between 4 and 8 mV (Fig. 2*E*). These effects put into context the remarkable distribution in ΔΨ under normal glucose, indicating that ΔΨ heterogeneity is a significant cellular feature and of possible importance to β-cell physiology.

Given the wide baseline diversity in mitochondrial activity, fuel metabolism may involve either general upregulation in mitochondrial activity or selective upregulation of either low- or high-active mitochondrial subpopulations. We observed mitochondrial ΔΨ heterogeneity to markedly decrease in response to both glucose and MeS (Fig. 2*D*). This effect is consistent with recruitment of low-active mitochondria to the hyperpolarized state. We propose that some mitochondria with lower activity might serve as a metabolic reservoir, with the ability to be recruited by fuel exposure to increase ATP production and downstream insulin secretion, and might represent a therapeutic target for failing β-cells. Indeed, increased β-cell metabolic efficiency has been suggested as a potential site of future insulin-secreting drugs (35).

Prolonged elevated levels of glucose and FFA result in GLT, which we find associated with a higher degree of ΔΨ heterogeneity (Fig. 4). It has recently been reported that chronic hyperglycemia results in decreased interaction of glucokinase with mitochondria (36). This dissociation may be asynchronous and may result in uneven distribution of glycolitic intermediates and products, giving rise to the increased heterogeneity observed under GLT.

Although we grossly show metabolic heterogeneity in intact islets (Fig. 1*A*), further study is needed to determine whether the specific characteristics of dispersed β-cells described here apply to β-cells of the intact islet and in vivo.

Mechanisms for ΔΨ heterogeneity. To identify an underlying mechanism of ΔΨ heterogeneity in the β-cell, we undertook a systematic approach characterizing ΔΨ over time followed by examining key points along the mitochondrial metabolic pathway.

Diversity versus unsteadiness. When a snap-shot image of multiple mitochondria is examined, unsynchronized changes in ΔΨ could appear as heterogeneity. We explored this possibility by tracking β-cell mitochondria over time and found that ΔΨ in mitochondria remain stable during periods of at least 20 min (Fig. 3*A*). Parallel observations were made in INS-1 cells (online supplement, Fig. S3*C–E*). This analysis additionally accounts for error associated with the definition of a mitochondrion's boundaries (27). PA-GFP_{mt} reliably identifies bordered matrix volumes, assuring that mitochondrial clusters do not dilute subtle changes in ΔΨ occurring in a single mitochondrion. We have previously reported ΔΨ oscillations in β-cells to be minute in comparison to glucose-induced hyperpolarization (5). These observations also suggest that oscillations at the level of the individual mitochondrion, if they exist, have a magnitude within the noise level, i.e., 1.6 mV.

Mitochondrial flickering is a phenomenon of rapid changes in mitochondrial membrane potential that result from transient openings of the permeability transition pore during apoptosis (30). The flickering is accompanied by the reversal of F1FO-ATPsynthase and the appearance of ATP-hydrolyzing mitochondria (37). Given the stable ΔΨ in mitochondria (online supplement, Fig. S3*D* and *E*) and the sparcity of ATP-hydrolyzing mitochondria, flickering is an unlikely explanation for the heterogeneity, both in normal conditions and under GLT (Fig. 4). In addition, mitochondrial swelling, a phenomenon associated with damage and apoptosis, was not observed (online supplement, Fig. S2*A* and *B*).

Fuel distribution. Pyruvate has been reported to be localized to subcellular domains, possibly due to differential distribution of glycolytic enzymes (38). To determine the implication of this distribution on ΔΨ heterogeneity, we compared ΔΨ changes in the presence of glucose and MeS. Bypassing upstream glucose metabolism with MeS would result in more pronounced decrease in ΔΨ heterogeneity if intracellular fuel distribution indeed impacts ΔΨ heterogeneity. That ΔΨ response was equivalent for both fuel types points to other mechanisms as underlying mitochondrial metabolic heterogeneity (Fig. 2*E*). In addition, mitochondrial localization did not affect ΔΨ, further suggesting that fuel distribution is not contributing to the observed heterogeneity in ΔΨ.

BAD/glucokinase. Mitochondrial metabolism depends on import of fuels, such as pyruvate from glycolysis or acyl-CoA derived from fatty acids. Mitochondrial glucokinase resides in a complex with the BCL-2 family member BAD (13) and may control mitochondrial metabolism through creation of an ADP-rich microenvironment. Our finding that $BAD^{-/-}$–dispersed β-cells exhibit a more narrow distribution range of ΔΨ heterogeneity suggests that the WT cells may have a heterogeneous distribution or activity of mitochondrial associated glucokinase (Fig. 4). It has been argued that acute glucose exposure mediates association of mitochondria with glucokinase (39). While such a process is consistent with the ΔΨ fuel response observed here, it has not been corroborated in other studies (40). Recently, a specific plant hexokinase (HXK1), mutated to lack catalytic activity, was shown to still support various signaling functions, thus uncoupling its glucose sensing and subsequent signaling from glucose metabolism (41). This suggests that BAD-glucokinase association regulates mitochondrial activity at low glucose

concentrations, while at stimulatory glucose levels this effect is absent or bypassed.

UCP2. It has been reported that UCP2 is induced as well as activated by FFA or ROS and thereby acts as the $\Delta\Psi$ rheostat (15,16). Thus, if different mitochondria experience different levels of ROS or have different access to FFA, it is expected that UCP2 would be activated and $\Delta\Psi$ might fall in a heterogeneous manner. However, we found no difference in the level of $\Delta\Psi$ heterogeneity (or its response to glucose between $UCP2^{-/-}$ and WT cells (Fig. 4). This indicates that UCP2 plays no role in the regulation of $\Delta\Psi$ heterogeneity. Thus, similar to previous reports in Chinese hamster ovary cells (42), these results do not support a role for UCP2 as a $\Delta\Psi$ rheostat in primary dispersed β-cells.

ATP-hydrolyzing mitochondria. A mitochondrion may under some circumstances reverse its F1FO-ATPsynthase activity and hydrolyze ATP to maintain its $\Delta\Psi$, e.g., during ischemia (43). Such mitochondria have reduced $\Delta\Psi$ and may thus contribute to $\Delta\Psi$ heterogeneity. To unmask ATP-hydrolyzing mitochondria, we used OM, an inhibitor of F1FO-ATPsynthase, and found that they constitute only a minor fraction of the mitochondrial population (Fig. 3*C*). That $\Delta\Psi$ heterogeneity decreases with OM (Fig. 2*B*) similarly to glucose further supports their relative scarceness. We therefore conclude ATP-hydrolyzing mitochondria to be an insignificant contributor to the level of $\Delta\Psi$ heterogeneity. Moreover, this finding indicates that fuel as well as oxygen is evenly accessible to mitochondria throughout the cell, since deficiency in these would be expected to reverse F1FO-ATPsynthase function in order to maintain $\Delta\Psi$.

To determine the contribution of artifacts to the observed heterogeneity, a systematic analysis of potential sources of noise was examined. These tests indicated that dispersion of cells had little or no contribution to heterogeneity. Imaging procedures have been estimated to contribute a maximum of 1.6 mV SD of one mitochondrion. That would translate into 1.97 SD for an imaging section with ~100 mitochondria, a value that should be considered as the noise of the methodology.

Other mechanisms, not examined here, may contribute to $\Delta\Psi$ heterogeneity. These include matrix Ca^{2+} levels, reported to regulate activity of Kreb's cycle dehydrogenases (44), generation of ROS and mitochondrial fusion and fission events (45).

ACKNOWLEDGMENTS

This work was supported by National Institutes of Health grants 5R01HL071629, 1R21DK070303, 1R01DK074778, 22RO1DK35914, and P41 RR001395. Confocal microscope was acquired by P30 NS047243, P30DKDK34928NSF, and National Science Foundation Grant DBI-0215829.

We thank David Nicholls, Dani Dagan, Anders Tengholm, Israel Biran, Jude Deeney, Keith Tornheim, Gordon Yaney, Esthere Luc, Steve Katz, Sarah Haigh, Alvaro Elorza, Gil Walzer, Peter Smith, and Channing Yu for helpful discussions; Louis Kerr, Craig Lassy, Jim Seams, Alenka Lovy-Wheeler, Lai Ding, Rob Jackson, and Tufts New England Medical Center, Center for Gastroenterology Research on Absorptive and Secretory Processes center for excellent technical support and advice.

REFERENCES

1. Duchen MR: Roles of mitochondria in health and disease. *Diabetes* 53 (Suppl. 1):S96–S102, 2004
2. Lowell BB, Shulman GI: Mitochondrial dysfunction and type 2 diabetes. *Science* 307:384–387, 2005
3. Antinozzi PA, Ishihara H, Newgard CB, Wollheim CB: Mitochondrial metabolism sets the maximal limit of fuel-stimulated insulin secretion in a model pancreatic beta cell: a survey of four fuel secretagogues. *J Biol Chem* 277:11746–11755, 2002
4. Chan CB, De Leo D, Joseph JW, McQuaid TS, Ha XF, Xu F, Tsushima RG, Pennefather PS, Salapatek AM, Wheeler MB: Increased uncoupling protein-2 levels in β-cells are associated with impaired glucose-stimulated insulin secretion: mechanism of action. *Diabetes* 50:1302–1310, 1999
5. Heart E, Corkey RF, Wikstrom JD, Shirihai OS, Corkey BE: Glucose-dependent increase in mitochondrial membrane potential, but not cytoplasmic calcium, correlates with insulin secretion in single islet cells. *Am J Physiol Endocrinol Metab* 290:143–148, 2006
6. Nicholls DG: Mitochondrial membrane potential and aging. *Aging Cell* 3:35–40, 2004
7. Collins TJ, Berridge MJ, Lipp P, Bootman MD: Mitochondria are morphologically and functionally heterogeneous within cells. *EMBO J* 21:1616–1627, 2002
8. Kuznetsov AV, Schneeberger S, Renz O, Meusburger H, Saks V, Usson Y, Margreiter R: Functional heterogeneity of mitochondria after cardiac cold ischemia and reperfusion revealed by confocal imaging. *Transplantation* 77:754–756, 2004
9. Smiley ST, Reers M, Mottola-Hartshorn C, Lin M, Chen A, Smith TW, Steele GD Jr, Chen LB: Intracellular heterogeneity in mitochondrial membrane potentials revealed by a J-aggregate-forming lipophilic cation JC-1. *Proc Natl Acad Sci U S A* 88:3671–3675, 1991
10. Diaz G, Setzu MD, Zucca A, Isola R, Diana A, Murru R, Sogos V, Gremo F: Subcellular heterogeneity of mitochondrial membrane potential: relationship with organelle distribution and intercellular contacts in normal, hypoxic and apoptotic cells. *J Cell Sci* 112:1077–1084, 1999
11. Salvioli S, Dobrucki J, Moretti L, Troiano L, Fernandez MG, Pinti M, Pedrazzi J, Franceschi C, Cossarizza A: Mitochondrial heterogeneity during staurosporine-induced apoptosis in HL60 cells: analysis at the single cell and single organelle level. *Cytometry* 40:189–197, 2000
12. Kirischuk S, Neuhaus J, Verkhratsky A, Kettenmann H: Preferential localization of active mitochondria in process tips of immature retinal oligodendrocytes. *Neuroreport* 6:737–741, 1995
13. Danial NN, Gramm CF, Scorrano L, Zhang CY, Krauss S, Ranger AM, Datta SR, Greenberg ME, Licklider LJ, Lowell BB, Gygi SP, Korsmeyer SJ: BAD and glucokinase reside in a mitochondrial complex that integrates glycolysis and apoptosis. *Nature* 424:952–956, 2003
14. Krauss S, Zhang CY, Lowell BB: The mitochondrial uncoupling-protein homologues. *Nat Rev Mol Cell Biol* 6:248–261, 2005
15. Boss O, Hagen T, Lowell BB: Uncoupling proteins 2 and 3: potential regulators of mitochondrial energy metabolism. *Diabetes* 49:143–156, 2000
16. Chan CB, Saleh MC, Koshkin V, Wheeler MB: Uncoupling protein 2 and islet function. *Diabetes* 53 (Suppl. 1):S136–S142, 2004
17. Zhang CY, Baffy G, Perret P, Krauss S, Peroni O, Grujic D, Hagen T, Vidal-Puig AJ, Boss O, Kim YB, Zheng XX, Wheeler MB, Shulman GI, Chan CB, Lowell BB: Uncoupling protein-2 negatively regulates insulin secretion and is a major link between obesity, beta cell dysfunction, and type 2 diabetes. *Cell* 105:745–755, 2001
18. Joseph JW, Koshkin V, Zhang CY, Wang J, Lowell BB, Chan CB, Wheeler MB: Uncoupling protein 2 knockout mice have enhanced insulin secretory capacity after a high-fat diet. *Diabetes* 51:3211–3219, 2002
19. Chan CB, MacDonald PE, Saleh MC, Johns DC, Marban E, Wheeler MB: Overexpression of uncoupling protein 2 inhibits glucose-stimulated insulin secretion from rat islets. *Diabetes* 48:1482–1486, 2001
20. Ranger AM, Zha J, Harada H, Datta SR, Danial NN, Gilmore AP, Kutok JL, Le Beau MM, Greenberg ME, Korsmeyer SJ: Bad-deficient mice develop diffuse large B cell lymphoma. *Proc Natl Acad Sci U S A* 100:9324–9329, 2003
21. Arsenijevic D, Onuma H, Pecqueur C, Raimbault S, Manning BS, Miroux B, Couplan E, ves-Guerra MC, Goubern M, Surwit R, Bouillaud F, Richard D, Collins S, Ricquier D: Disruption of the uncoupling protein-2 gene in mice reveals a role in immunity and reactive oxygen species production. *Nat Genet* 26:435–439, 2000
22. Roduit R, Morin J, Masse F, Segall L, Roche E, Newgard CB, Assimacopoulos-Jeannet F, Prentki M: Glucose down-regulates the expression of the peroxisome proliferator-activated receptor-alpha gene in the pancreatic beta-cell. *J Biol Chem* 275:35799–35806, 2000
23. Quesada I, Todorova MG, Soria B: Different metabolic responses in alpha,

beta and delta-cells of the islet of Langerhans monitored by redox confocal microscopy. *Biophys J* 90:2641–2650, 2006
24. Holz GG 4th, Kuhtreiber WM, Habener JF: Pancreatic beta-cells are rendered glucose-competent by the insulinotropic hormone glucagon-like peptide-1. *Nature* 361:362–365, 1993
25. Wang X, Zeng W, Murakawa M, Freeman MW, Seed B: Episomal segregation of the adenovirus enhancer sequence by conditional genome rearrangement abrogates late viral gene expression. *J Virol* 74:11296–11303, 2000
26. de Vargas LM, Sobolewski J, Siegel R, Moss LG: Individual beta cells within the intact islet differentially respond to glucose. *J Biol Chem* 272:26573–26577, 1997
27. Twig G, Graf SA, Wikstrom JD, Mohamed H, Haigh SE, Elorza AG, Deutsch M, Zurgil N, Reynolds N, Shirihai OS: Tagging and tracking individual networks within a complex mitochondrial web using photoactivatable GFP. *Am J Physiol Cell Physiol* 291:176–184, 2006
28. Duchen MR, Surin A, Jacobson J: Imaging mitochondrial function in intact cells. *Methods Enzymol* 361:353–389, 2003
29. Ehrenberg B, Montana V, Wei MD, Wuskell JP, Loew LM: Membrane potential can be determined in individual cells from the nernstian distribution of cationic dyes. *Biophys J* 53:785–794, 1988
30. O'Reilly CM, Fogarty KE, Drummond RM, Tuft RA, Walsh JV Jr: Quantitative analysis of spontaneous mitochondrial depolarizations. *Biophys J* 85:3350–3357, 2003
31. Pendergrass W, Wolf N, Poot M: Efficacy of MitoTracker Green and CMXrosamine to measure changes in mitochondrial membrane potentials in living cells and tissues. *Cytometry* 61:A162–A169, 2004
32. Brand MD, Esteves TC: Physiological functions of the mitochondrial uncoupling proteins UCP2 and UCP3. *Cell Metab* 2:85–93, 2005
33. Mitchell P: Vectorial chemistry and the molecular mechanics of chemiosmotic coupling: power transmission by proticity. *Biochem Soc Trans* 4:399–430, 1976
34. Ishihara N, Jofuku A, Eura Y, Mihara K: Regulation of mitochondrial morphology by membrane potential, and DRP1-dependent division and FZO1-dependent fusion reaction in mammalian cells. *Biochem Biophys Res Commun* 301:891–898, 2003
35. Henquin JC: Pathways in beta-cell stimulus-secretion coupling as targets for therapeutic insulin secretagogues. *Diabetes* 53 (Suppl. 3):48–58, 2004
36. Kim WH, Lee JW, Suh YH, Hong SH, Choi JS, Lim JH, Song JH, Gao B, Jung MH: Exposure to chronic high glucose induces β-cell apoptosis through decreased interaction of glucokinase with mitochondria: downregulation of glucokinase in pancreatic β-cells. *Diabetes* 54:2602–2611, 2005
37. Polster BM, Kinnally KW, Fiskum G: BH3 death domain peptide induces cell type-selective mitochondrial outer membrane permeability. *J Biol Chem* 276:37887–37894, 2001
38. Margineantu DH, Brown RM, Brown GK, Marcus AH, Capaldi RA: Heterogeneous distribution of pyruvate dehydrogenase in the matrix of mitochondria. *Mitochondrion* 1:327–338, 2002
39. Vanhoutte C, Sener A, Malaisse WJ: Subcellular distribution of hexokinase isoenzymes in pancreatic single beta cells exposed to digitonin after incubation at a low or high concentration of D-glucose. *Mol Cell Biochem* 175:131–136, 1997
40. Arden C, Harbottle A, Baltrusch S, Tiedge M, Agius L: Glucokinase is an integral component of the insulin granules in glucose-responsive insulin secretory cells and does not translocate during glucose stimulation. *Diabetes* 53:2346–2352, 2004
41. Moore B, Zhou L, Rolland F, Hall Q, Cheng WH, Liu YX, Hwang I, Jones T, Sheen J: Role of arabidopsis glucose sensor HXK1 in nutrient, light and hormonal signaling. *Science* 300:332–336, 2003
42. Mozo J, Ferry G, Studeny A, Pecqueur C, Rodriguez M, Boutin JA, Bouillaud F: Expression of UCP3 in CHO cells does not cause uncoupling but controls mitochondrial activity in the presence of glucose. *Biochem J* 393:431–439, 2006
43. Takeda Y, Perez-Pinzon MA, Ginsberg MD, Sick TJ: Mitochondria consume energy and compromise cellular membrane potential by reversing ATP synthetase activity during focal ischemia in rats. *J Cereb Blood Flow Metab* 24:986–992, 2004
44. McCormack JG, Halestrap AP, Denton RM: Role of calcium ions in regulation of mammalian intramitochondrial metabolism. *Physiol Rev* 70:391–425, 1990
45. Chen H, Chan DC: Emerging functions of mammalian mitochondrial fusion and fission. *Hum Mol Genet* 14:283–389, 2005